Plant Physiol. (1997) 114: 927–935

Antisense Expression of the Peptide Transport Gene *AtPTR2-B* Delays Flowering and Arrests Seed Development in Transgenic Arabidopsis Plants[1]

Wei Song, Serry Koh, Mihaly Czako, Laszlo Marton, Eliana Drenkard, Jeffrey M. Becker, and Gary Stacey*

Center for Legume Research (W.S., S.K., G.S.), Department of Microbiology (W.S., S.K., J.M.B., G.S.), and Ecology and Evolutionary Biology (G.S.), The University of Tennessee, Knoxville, Tennessee 37996–0845; Department of Biological Sciences, The University of South Carolina, Columbia, South Carolina 29208 (M.C., L.M.); and Department of Genetics, Harvard Medical School, and Department of Molecular Biology, Massachusetts General Hospital, Boston, Massachusetts 02114 (E.D.)

Previously, we identified a peptide transport gene, *AtPTR2-B*, from *Arabidopsis thaliana* that was constitutively expressed in all plant organs, suggesting an important physiological role in plant growth and development. To evaluate the function of this transporter, transgenic Arabidopsis plants were constructed expressing antisense or sense *AtPTR2-B*. Genomic Southern analysis indicated that four independent antisense and three independent sense *AtPTR2-B* transgenic lines were obtained, which was confirmed by analysis of the segregation of the kanamycin resistance gene carried on the T-DNA. RNA blot data showed that the endogenous *AtPTR2-B* mRNA levels were significantly reduced in transgenic leaves and flowers, but not in transgenic roots. Consistent with this reduction in endogenous *AtPTR2-B* mRNA levels, all four antisense lines and one sense line exhibited significant phenotypic changes, including late flowering and arrested seed development. These phenotypic changes could be explained by a defect in nitrogen nutrition due to the reduced peptide transport activity conferred by *AtPTR2-B*. These results suggest that *AtPTR2-B* may play a general role in plant nutrition. The *AtPTR2-B* gene was mapped to chromosome 2, which is closely linked to the restriction fragment length polymorphism marker m246.

Peptide transport systems mediate the uptake of small peptides in an energy-dependent manner (Payne and Smith, 1994). These transport systems have been extensively studied in prokaryotes, fungi, and animals (Becker and Naider, 1980, 1995; Ganapathy and Leibach, 1991; Payne and Smith, 1994). In bacteria peptide transport has been found to be mainly involved in utilizing peptides as sources of nitrogen and carbon. A few reports have shown that the peptide transport system is also involved in other cellular processes, such as cell wall recycling (Goodell and Higgins, 1987), chemotaxis (Manson et al., 1986), and sporulation (Mathiopoulos et al., 1991; Perego et al., 1991). In animals peptide transport has been shown to mediate the absorption of small peptides in the small intestine (Matthews, 1991), suggesting a vital role in protein nutrition. In addition, some peptide analogs, such as β-lactam antibiotics and bestatin, have been found to be transported by this transport system (Brandsch et al., 1994), implying clinical applications of the intestinal peptide transport system.

There is no clear picture of the physiological significance of peptide transport in planta. It has been reported that isolated scutella from germinating barley (*Hordeum vulgare*) seeds have the ability to transport small peptides that are released from endosperm into the embryo, and are subsequently hydrolyzed to amino acids for growth (Sopanen et al., 1977; Higgins and Payne, 1978; Salmenkallio and Sopanen, 1989). Also, the isolation of plant peptide-conjugated hormones (Andreae et al., 1955; Winter and Thimann, 1966) implies the possible involvement of a peptide transport system in the regulation of plant hormone activity (Higgins and Payne, 1982). Peptide transport systems may be involved in the movement of such hormone-peptide conjugates within the plant. In addition, several phytotoxins produced by plant pathogens are modified peptides (Willis et al., 1991). It is possible that peptide transport systems could transport small peptide phytotoxins such as the dipeptide tabtoxin, produced by *Pseudomonas syringae* pv *tabaci* (Gross, 1991), or the tripeptide phaseolotoxin, produced by *Pseudomonas phaseolicola* (Mitchell, 1976; Mitchell and Bieleski, 1977). Recently, we have isolated two unique peptide transport genes from *Arabidopsis thaliana*. However, only one of these genes, *AtPTR2-B*, accumulates mRNA to a significant level. Our results indicate that *AtPTR2-B* is highly expressed in siliques, flowers, roots, leaves, stems, and germinating seeds (Song et al., 1996), suggesting an important role in plant growth and development.

To study the in vivo role of the peptide transport gene *AtPTR2-B* in plants, we created transgenic Arabidopsis plants expressing antisense or sense constructs of *AtPTR2-B* under the control of the cauliflower mosaic virus 35S RNA

[1] This research was funded by grant no. 9502661 from the U.S. Department of Agriculture.

*Corresponding author; e-mail gstacey@utk.edu; fax 1–423–974–4007.

Abbreviations: BA6, BA8, BA21, and BA27, independent transgenic *Arabidopsis thaliana* lines expressing *At*PTR2B in an antisense orientation; BS1, BS2, and BS9, independent transgenic *A. thaliana* lines expressing *At*PTR2B in a sense orientation; cM, centimorgan.

promoter. A number of transgenic plants with reduced *AtPTR2-B* mRNA accumulation were identified. Consistently, these transgenic plants exhibited delayed flowering and an arrest of seed development.

MATERIALS AND METHODS

Construction of Binary Ti Plasmids Containing Antisense or Sense cDNAs

The plasmids containing the truncated *AtPTR2-B* gene were constructed starting with a pBluescript SK-2B containing the complete cDNA clone of *AtPTR2-B* (Song et al., 1996). To clone *AtPTR2-B* into the *Xba*I site of the plant expression vector pGA941 (with the 35s RNA promoter sequence and kanamycin resistance gene *nptII* [An et al., 1988; Czako and An, 1991]), *AtPTR2-B* was subcloned sequentially into pUC19 and pBluescript SK. The *Sac*I-*Xba*I fragment of *AtPTR2-B* from pBluescript SK-2B, which has a 100-bp deletion of the coding region and lacks 230 bp from the 3′ noncoding region of the *AtPTR2-B* cDNA, was inserted between the *Sac*I and *Xba*I restriction sites of pUC19. The *Eco*RI and *Sal*I fragment containing *AtPTR2-B* was then excised from pUC19 and cloned into pBluescript SK. The *Xba*I fragment containing *AtPTR2-B* was liberated and inserted into the *Xba*I site of pGA941. The sense and antisense orientation of *AtPTR2-B* in pGA941 was determined by restriction enzyme digestion analysis. The sense gene construct was designated pGA-2BS and the antisense gene construct was designated pGA-2BA.

Transformation of *Agrobacterium tumefaciens*

The pGA941 plasmids containing the antisense or sense *AtPTR2-B* construct were transformed into *Escherichia coli* MC1000 (Casadaban and Cohen, 1980; this strain gives a higher efficiency of transformation than other strains tested), and transformants were selected on Luria broth medium containing kanamycin (10 μg/mL) and tetracycline (3 μg/mL) (Czako and An, 1991). The plasmids were then isolated and transformed into *A. tumefaciens* strain EHA105 (Hood et al., 1993) by electroporation (Sambrook et al., 1989). Transformants were selected on YEP medium (for 1 L, 10 g of Bacto-peptone, 10 g of Bacto-yeast extract, 5 g of NaCl, and 15 g of agar, pH 7.0) containing tetracycline (3 μg/mL), kanamycin (10 μg/mL), and rifampicin (25 μg/mL). The plasmids were isolated from the *A. tumefaciens* transformants by the alkaline lysis method (Sambrook et al., 1989) and then digested with *Xba*I, *Bam*HI, or *Eco*RI to confirm that no changes occurred in the plasmid DNA.

Plant Transformation and Analysis of Transgenic Plants

Transformation of *Arabidopsis thaliana* was performed by root-explant transformation as previously described (Marton and Browse, 1991). The regenerated plants from *A. tumefaciens*-treated roots were selected on kanamycin-containing medium (75 μg/mL). Transgenic plants were transferred to soil and grown in a Percival plant growth chamber (MFG Co., Boone, IA) (21–24°C, 16 h of light and 8 h of dark). Genomic DNA was isolated by the cetyltrimethylammonium bromide method (Rogers, 1985) and digested with *Bam*HI for detection of the transgenic sense *AtPTR2-B* or with *Eco*RI for detection of the transgenic antisense *AtPTR2-B*. Genomic Southern analysis was done as described in Sambrook et al. (1989). A ^{32}P-labeled *AtPTR2-B*-specific DNA probe (*Not*I fragment from pBluescript SK-2B) was obtained using a random hexamer-primed labeling kit (Promega). For northern analysis, total RNA was extracted from leaves, roots, and flowers using the TRIzol Reagent kit, (GIBCO-BRL). To measure the mRNA level of the host gene *AtPTR2-B* in plants, a 330-bp *Sac*I/*Not*I fragment (from pBluescript SK-2B) derived from the 3′end of *AtPTR2-B* was radiolabeled as a probe. The transgenic *AtPTR2-B* gene lacks this sequence. As a control for RNA loading, membranes were hybridized with a 28S rRNA-encoding cDNA probe (Takaiwa et al., 1984). The amount of the endogenous *AtPTR2-B* mRNA in the samples was determined by densitometry analysis of the autoradiograms using a computing densitometer (model 325 E, ImageQuant, Molecular Dynamics, Sunnyvale, CA; quantitation by volume integration). The intensity of a mRNA signal was expressed as a percentage of the wild-type signal occupied among all signals compared. In every case, signals were corrected for RNA loading based on hybridization with a 28S rDNA probe.

Seed Germination and Segregation of Kanamycin Resistance

Seeds were sown to a density of 50 to 100 seeds per plate on G-H medium (Marton and Browse, 1991; for 1 L, 3.1 g of Gamborg's B_5 salts, 3 mL of 6% [w/v] KH_2PO_4, 30 g of Suc, and 10 g of agar, pH 5.6–5.8). Parafilm-sealed plates were placed at room temperature in the dark for 2 d before transferring to the growth chamber, with a photoperiod of 16 h of light and 8 h of dark. Plates lacking kanamycin selection were used to measure germination frequency. Seedlings were individually transferred aseptically to plates containing 75 μg/mL kanamycin, sealed, and placed back in the light. After 10 d plates were scored for kanamycin sensitivity, as characterized by chlorosis and death.

Microscopic Analysis

For scanning electron microscopy, green siliques were dissected under the stereomicroscope and fixed in 3% glutaraldehyde in 0.025 M sodium phosphate buffer (pH 7.0) at 4°C for 12 to 16 h. The samples were then rinsed in the same buffer briefly and postfixed in 1% OsO_4 in 0.05 M sodium cacodylate buffer (pH 7.0) at 4°C for 12 to 24 h. After rinsing with 0.025 M sodium phosphate buffer (pH 7.0), the samples were dehydrated in a graded ethanol series (25–100%) at 4°C. The treated siliques were critical-point-dried using liquid CO_2 and mounted on scanning electron microscopy stubs. The mounted specimens were coated with gold:palladium (60%/40%) and observed with a scanning electron microscope (Autoscan, ETEC, Hayward, CA) at 20 kV. Photographs were taken using type 55 Polaroid film.

To observe embryo development at different stages, stereomicroscopic analysis was performed. Seeds were removed from siliques at the different stages of development, dissected and examined using a stereomicroscope with the magnifications of 10× to 15×.

Phenotypic Analysis of Transgenic Plants

The average weight per seed was determined by weighing 5 samples of 100 seeds each, and the average seed number per silique was measured by counting the seed number of 30 siliques. The length of siliques was determined by measuring 30 siliques for each transgenic line.

Seed development in siliques was analyzed by dissecting the siliques and examining the seeds under a dissecting stereomicroscope (10×).

Chromosome Number

The chromosome number was determined by aceto-orcein staining of flattened root tips (Berlyn and Miksche, 1976). Briefly, young (2–3 weeks old) seedlings grown on G-H medium were incubated in 0.15% colchicine for 3 h at 22°C. Plants were fixed in an ethanol:glacial acetic acid (3:1, v/v) solution for 1 h at 22°C. Fixation was repeated overnight at 4°C, and these samples were gradually rehydrated from 50% ethanol to water. Samples were transferred into a 45% aceto-orcein, 1 N HCl solution for 5 to 10 min and placed onto a new glass slide in a drop of dilute 45% aceto-orcein stain. Root tips were removed and flattened as previously described (Berlyn and Miksche, 1976). The chromosome preparation was analyzed by a phase-contrast microscope (1000X, Zeiss) and photographed using T-MAX 400 film (Kodak).

Mapping

Genomic DNA was isolated from *A. thaliana* ecotypes Landsberg erecta and Columbia and digested separately with the restriction enzyme *Bam*HI, *Bcl*I, *Hpa*I, or *Xba*I. The digested genomic DNA was then subjected to electrophoresis and blotted to a neutral nylon membrane (Sigma). Southern blots were hybridized with a ^{32}P-labeled *AtPTR2-B*-specific cDNA probe to detect a polymorphism between the two ecotypes. Polymorphisms were detected for *Hpa*I, *Bcl*I, and *Xba*I restriction enzymes, and *Xba*I was selected for the mapping.

AtPTR2-B was mapped using 98 recombinant inbred lines generated from the cross between the Columbia (Col-0) and Landsberg erecta ecotypes (Lister and Dean, 1993). The *AtPTR2-B*-specific cDNA probe was prepared using a random-priming kit. Blots with *Xba*I-digested DNA from the 98 recombinant inbred lines were prepared as described previously (Ausubel et al., 1995). The filters (GeneScreen Plus, DuPont-New England Nuclear) were hybridized and washed according to the manufacturer's recommendations, exposed to phosphor imager screens (Molecular Dynamics) and developed. The segregation of the marker in the recombinant inbred lines was followed as previously described by Lister and Dean (1993).

RESULTS

Detection of Transgenic Antisense and Sense DNA

To determine whether the genomic DNA of the putative transformants contained the transgene DNA, genomic Southern-blot hybridization was carried out using a *AtPTR2-B*-specific probe. Because the wild-type genomic DNA generated a single band when digested with *Eco*RI or *Bam*HI, the transgene *AtPTR2-B* was distinguished from the endogenous *AtPTR2-B* due to the different sizes of their genomic DNA fragments (Fig. 1). Screening 10 antisense and sense transformants, respectively, generated four independent antisense lines, namely BA6, BA8, BA21, and BA27, and three independent sense lines, BS1, BS2 and BS9. BA8, BA21, and BS1 contained one copy of *AtPTR2-B*-containing T-DNA, whereas BA6, BA27, BS2, and BS9 contained two copies of T-DNA (Fig. 1). The copy number of T-DNA was further confirmed by the segregation analysis of kanamycin resistance conferred by the *nptII* gene carried within T-DNA (data not shown).

Decreased Levels of *AtPTR2-B* mRNA because of Antisense Gene Inhibition

The effect of *AtPTR2-B* antisense gene expression upon the steady-state levels of the endogenous *AtPTR2-B* mRNA was analyzed. Total RNA was extracted from the leaves, roots, and flowers of transgenic plants. The RNA was probed with a 330-bp *Sac*I/*Not*I fragment of *AtPTR2-B*. This fragment is absent from the transgene and will only detect the endogenous mRNA. As shown in Figure 2, *AtPTR2-B* mRNA levels were significantly reduced in leaves (Fig. 2A). Similar results (30–80% reduction) were found for mRNA extracted from flowers of the transformed lines containing the antisense construct (data not shown). The reduced

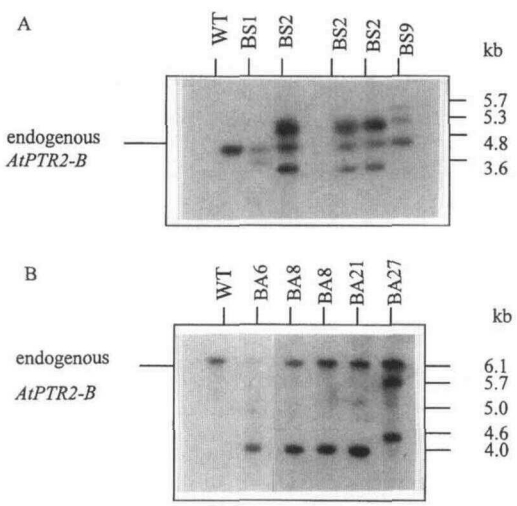

Figure 1. Southern analysis of antisense and sense *AtPTR2-B* plant DNAs hybridized with a *AtPTR2-B*-specific probe. A, The genomic Southern blot of sense plants digested with *Bam*HI. Lane 1, Wild type (WT); lane 2, BS1; lanes 3, 4, and 5, BS2; lane 6, BS9. B, The genomic Southern blot of antisense plants digested with *Eco*RI. Lane 1, Wild type (WT); lane 2, BA6; lanes 3 and 4, BA8; lane 5, BA21; lane 6, BA27.

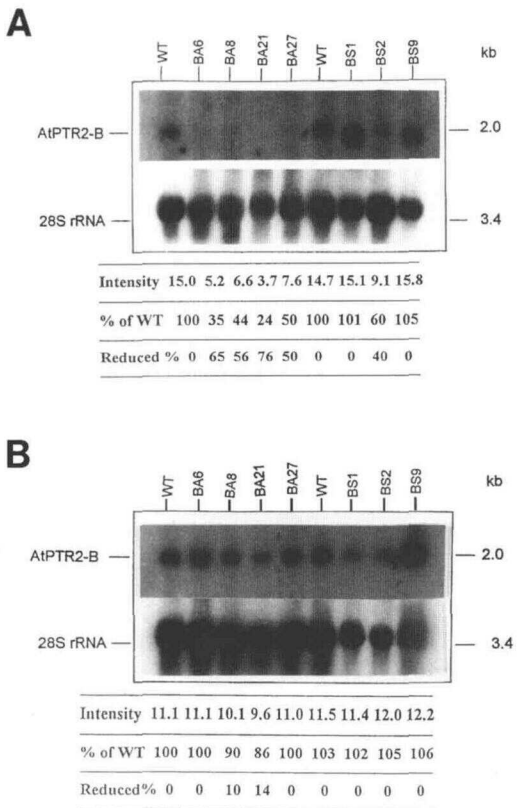

Figure 2. Northern analysis of endogenous *AtPTR2-B* mRNA in leaves (A) and roots (B) from antisense and sense Arabidopsis plants. Twenty micrograms of total RNA from the wild-type and transgenic plants was separated on formaldehyde/agarose gels, blotted onto nitrocellulose membranes, and probed with a ^{32}P-labeled 330 bp of *AtPTR2-B* cDNA. Approximate transcript size is given to the right. The membrane was reprobed with a 28S rRNA-encoding DNA probe to ensure equal loading in each well. The intensity of the signals was measured using a densitometer, and the data were normalized to compare the difference in signal intensity among the samples. Lane 1, Wild type (WT); lane 2, BA6; lane 3, BA8; lane 4, BA21; lane 5, BA27; lane 6, wild type (WT); lane 7, BS1; lane 8, BS2; lane 9, BS9.

mRNA levels varied among these transgenic lines, with BA21 showing the most significant reduction in *AtPTR2-B* mRNA (60–80%). Surprisingly, *AtPTR2-B* mRNA levels were not significantly reduced (approximately 10%) in extracts of the root tissue (Fig. 2B).

Endogenous *AtPTR2-B* mRNA Levels Vary among Plants Transformed with the Sense Construct

The RNA gel-blot data, as shown in Figure 2, indicate that the endogenous *AtPTR2-B* mRNA in leaves was reduced approximately 40% in line BS2, as compared with the wild type. This reduction (30–40%) was also found in the *AtPTR2-B* mRNA levels from flowers (data not shown). In contrast, lines BS1 and BS9 showed wild-type levels of endogenous *AtPTR2-B* mRNA. We propose that reduction of *AtPTR2-B* expression in line BS2 is due to co-suppression (Dougherty and Parks, 1995). As shown below, consistent with this idea, the phenotypes of the BS2 line resemble that of the antisense transgenic plants.

Reduced Levels of *AtPTR2-B* mRNA Correlate with Delayed Flowering

One of the earliest phenotypic changes observed among the transgenic lines was late flowering (Fig. 3). Control wild-type plants and those transformed with the pGA941 vector alone started flowering after approximately 3 weeks of vegetative growth. In contrast, flowering of the antisense lines and the sense line BS2 was delayed for 7 to 15 d. The sense lines BS1 and BS9 flowered at the same time as the controls. Moreover, prior to initiating flowering, the late-flowering plants produced rosette leaves 3-fold larger than those of the controls (Table I), although the number of the rosette leaves was the same. After transition to flowering, the late-flowering lines generated bigger inflorescence stems and flowers, as well as more cauline leaves (data not shown). However, the flower structure of the late-flowering plants was similar to that of the controls.

Altmann et al. (1994) reported that a significant proportion (13–38%) of transgenic Arabidopsis plants obtained by

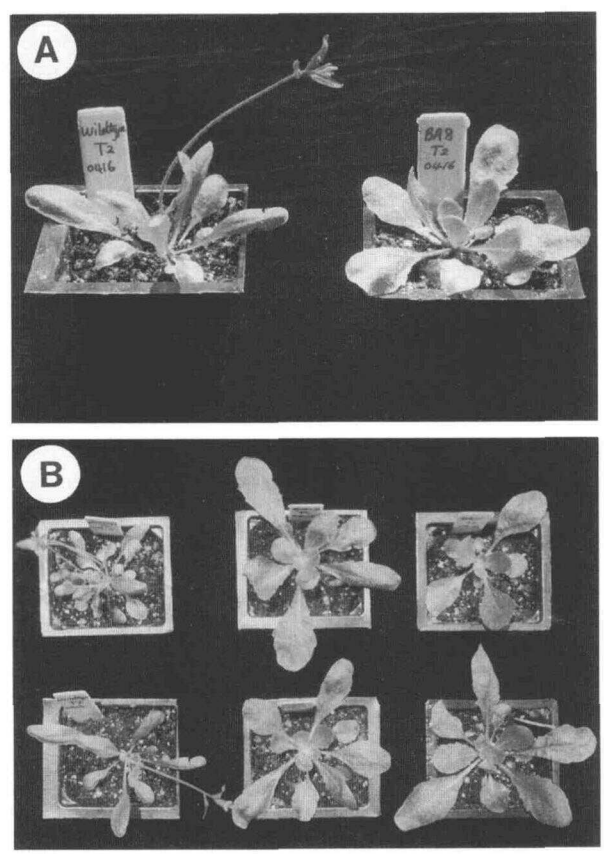

Figure 3. The late-flowering phenotype of *AtPTR2-B* transgenics. A, Left side shows the wild-type plant, whereas the right side shows the antisense BA8 line. B, The wild-type plant is the left plant on the bottom row, the vector control plant is the left plant on the top row, whereas the remaining plants represent individual antisense *AtPTR2-B* lines (middle top, BA8; middle bottom, BA6; right top, BA21; and right bottom, BA27).

Table I. *Leaf analysis of AtPTR2-B transgenics: T_2 plants*

Line[a]	Mean Leaf Weight[b]
	mg
Wild type	45.2 ± 6.5[c]
pGA941[d]	35.9 ± 14.8
AtPTR2-B antisense	
BA6	141.4 ± 21.6
BA8	106.3 ± 20.7
BA21	123.7 ± 22.2
BA27	106.3 ± 16.5
AtPTR2-B sense	
BS1	41.2 ± 7.2
BS2	135.2 ± 20.5
BS9	42.5 ± 8.5

[a] T_2 transgenic plants were obtained from T_1 seeds germinated on kanamycin-containing medium and then transferred to the soil. Therefore, all T_2 transgenic plants analyzed were homozygous or heterozygous and resistant to kanamycin. [b] Mean leaf weight of the *AtPTR2-B* transgenic lines BA6, BA8, BA21, BA27 and BS2 is significantly different from the mean leaf weight of wild-type and pGA941 vector controls ($t = 19.016$, $df = 18$, and $P < 0.001$), as well as different from the transgenic lines BS1 and BS9 ($t = 0.336$, $df = 18$, and $0.1 < P < 0.999$). A two-sample Student's *t* test was used to test for the significant differences between sample means (Steel and Torrie, 1980). [c] SD was derived from the average of 10 leaves taken from at least two independent plants for each line. [d] pGA941 vector control.

A. tumefaciens infection of root explants were tetraploid or aneuploid. The tetraploid transgenic plants obtained showed late flowering and larger leaves. Because these phenotypes were also found with our AtPTR2B transgenic plants, we sought to confirm the diploid ($2n = 10$; Heslop-Harrison and Maluszyuska, 1994) chromosome number of our *A. tumefaciens*-mediated transgenic plants. This analysis consistently showed 10 ± 3 chromosomes in flattened roots from the wild type and each of the transgenic plant lines (data not shown). We conclude that the phenotypes observed in the AtPTR2B plants are not due to tetraploidy but are the result of transgene expression.

Arrested Seed Development Correlates with Decreased *AtPTR2-B* mRNA Levels

As described above, peptide transport has been suggested to play an important nutritional role in supplying nitrogen to the plant embryo (Higgins and Payne, 1978). Our previous results indicate that *AtPTR2-B* mRNA is highly expressed in young siliques (Song et al., 1996), suggesting its role in seed development. Therefore, reduction of AtPTR2-B mRNA levels might affect seed maturation. To test this hypothesis, the reproductive organs (flowers and siliques) of the control and transgenic plants were examined. The transgenic flowers did not show any visible differences from those of the control, except for their slightly bigger size (data not shown). Table II shows that the transgenic lines produced siliques the same length as the controls, indicating that the reduction in *AtPTR2-B*

Table II. *Morphometric analysis of siliques and seeds of AtPTR2-B transgenics: T_2 plants*

Line[a]	Mean Silique Length[b]	Mean Seed No. per Silique[c]	Seed No. per cm of Silique Length[d]	Mean Weight per Seed[e]
	cm			*μg*
Wild type	1.2 ± 0.2[f]	40 ± 8[f]	33	14.4 ± 0.9[g]
pGA941	1.2 ± 0.2	45 ± 8	38	15.3 ± 0.7
AtPTR2-B antisense				
BA6	1.2 ± 0.1	22 ± 5	18	35.6 ± 0.6
BA8	1.2 ± 0.2	16 ± 7	13	36.2 ± 0.7
BA21	1.2 ± 0.2	21 ± 6	18	37.4 ± 0.6
BA27	1.2 ± 0.1	17 ± 7	14	34.0 ± 0.8
AtPTR2-B sense				
BS1	1.2 ± 0.2	34 ± 9	29	15.2 ± 0.8
BS2	1.2 ± 0.2	22 ± 7	18	27.6 ± 0.6
BS9	1.2 ± 0.2	37 ± 7	31	14.6 ± 0.6

[a] Seeds resulting from self-pollination of T_2 plants. [b] Mean silique length of *AtPTR2-B* transgenic lines is not significantly different from the mean silique length of wild-type and pGA941 vector controls ($t = 0$, $df = 58$, and $0.5 < P < 0.999$). A two-sample Student's *t* test was used to test for the significant differences between sample means (Steel and Torrie, 1980). [c] Mean seed number per silique of *AtPTR2-B* antisense transgenic lines and BS2 is significantly different from the mean seed number of wild-type and pGA941 vector controls ($t = 8.884$, $df = 58$, and $P < 0.001$), as well as different from transgenic lines BS1 and BS9 ($t = 1.546$, $df = 58$, and $0.5 < P < 0.999$). [d] Mean seed number per silique length of *AtPTR2-B* antisense transgenic lines and BS2 is significantly lower than the mean seed number per silique of wild-type and pGA941 vector controls, as well as different from transgenic lines BS1 and BS9. [e] Mean seed weight per seed of *AtPTR2-B* antisense transgenic lines and BS2 is significantly different from the mean seed weight per seed of wild-type and pGA941 vector controls ($t = 27.848$, $df = 8$, and $P < 0.001$), as well as different from the transgenic lines BS1 and BS9 ($t = 0.844$, $df = 8$, and $0.5 < P < 0.999$). [f] SD was derived from average of 30 siliques. [g] SD is average of five samples of 100 seeds each line.

mRNA did not appear to affect silique formation and growth. However, the seed number per silique was significantly decreased in the antisense plants and the sense plant BS2 when compared with that of the controls, implying that reduced *AtPTR2-B* mRNA expression affects seed development. In contrast, the sense plants BS1 and BS9, expressing normal levels of *AtPTR2-B* mRNA, produced a similar number of seeds per silique as the controls. The seed weight per seed was significantly greater in the antisense and BS2 lines when compared with the controls or the BS1 and BS9 lines. This suggests a similar import of nutrients into the transgenic and control siliques, which is then utilized in the antisense transgenic lines to produce fewer seeds.

The fact that the siliques formed by the transgenics and the controls were of the same length, but that fewer seeds were produced in the transgenics, suggests that silique elongation and seed development are independent events with regard to *AtPTR2-B* expression. To further address the role of *AtPTR2-B* in seed development, young and mature siliques were dissected and examined by stereomicroscopy and scanning electron microscopy. As shown in Figure 4A, the transgenic mature siliques contained healthy and aborted seeds, which were easily distinguished from each other by the differences in seed shape and size; the aborted seeds (shrinkage likely due to dehydration) were significantly smaller than the healthy seeds (Fig. 4B), and the early-developed seeds, such as heart-stage embryo-containing seeds in young siliques, did not show a significant difference in seed size and shape (data not shown). Table III summarizes the number of the healthy and aborted seeds per silique. Siliques on the control plants contained an average of 45 healthy seeds and 2 aborted seeds, but at least one-half of the seeds were aborted in siliques of the antisense lines and line BS2 (20 aborted seeds on average per silique).

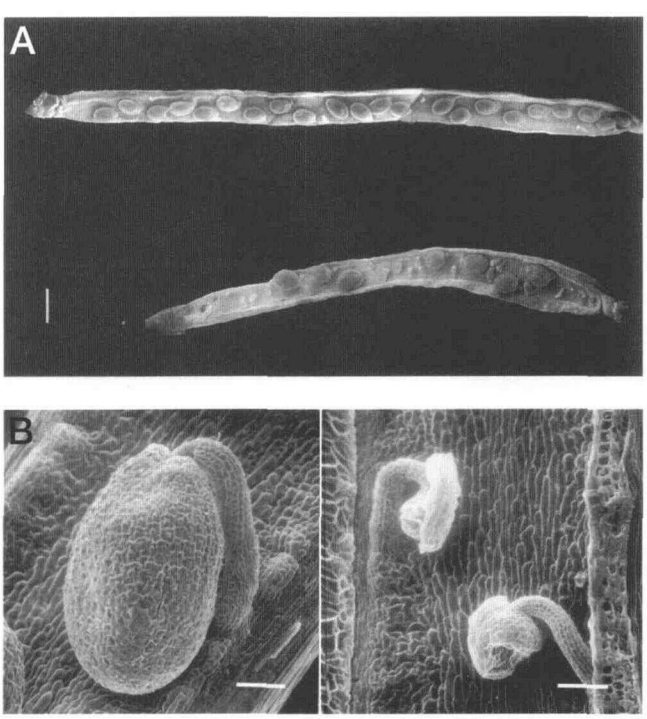

Figure 4. Scanning electron micrographs of siliques. A, Siliques formed on the wild-type (top) and BA21 transgenic line (bottom). The magnification is 13× (bar = 0.77 mm). B, Wild-type seeds (left) and aborted seeds (right) formed by the transgenic line BA21. The magnification is 125× (bar = 0.08 mm).

Mapping of *AtPTR2-B*

A *Xba*I polymorphism between Landsberg erecta and Columbia was used to map the *AtPTR2-B* gene, using the collection of recombinant inbred lines generated by Lister and Dean (1993). *AtPTR2-B* maps to chromosome 2 at 10.5 cM close to the RFLP marker m246 at 14.1 cM (Fig. 5; data are accessible at http://nasc.nott.ac.uk/new_ri_map.html).

DISCUSSION

In the past decades peptides and peptide-like compounds and their corresponding transport systems have received little attention in plants. However, several lines of evidence have demonstrated that peptide transport not only exists in plants, but may participate in central physiological processes such as nutrition. The finding of significant amounts of peptides and their putative transport among different organs, such as long distance transport via the phloem and xylem, suggest that there are peptide transporters present in the plasma membrane of these cells (Higgins and Payne, 1982). Moreover, plant cells presumably have different peptide transport systems to correspond to various peptides and their identified analogs, such as peptide-hormone conjugates (Klambt, 1960; Thurmann and Street, 1962; Bewley et al., 1986), phytotoxins (e.g. tabtoxin and phaseolotoxin; Walton, 1990; Willis et al., 1991), and the dialanine-based herbicide, bialaphos (Damm et al., 1993). Consistent with this idea, it was found that phaseolotoxin can be transported via the oligopeptide permease system in *E. coli* and *Salmonella typhimurium* (Staskawicz and Panopoulos, 1980).

Peptide transport so far has been characterized only in barley grains and broad bean leaf tissues. In barley seeds this process occurs in the scutellum tissue, which is responsible for the transport of peptides resulting from the hydrolysis of seed proteins in endosperm to the embryo (Sopanen et al., 1977; Higgins and Payne, 1978). Jamai et al. (1994) reported that a peptide transporter also exists in mature leaves from broad bean and that it may be responsible for the exchange of nitrogenous compounds. Our recent isolation of two unique Arabidopsis peptide transport genes, *AtPTR2-A* (Steiner et al., 1994) and *AtPTR2-B* (Song et al., 1996), provides direct evidence for the presence of peptide transporters in plants. Differences in kinetic characteristics and expression patterns further suggest that these two peptide transporters play different physiological roles in planta. The high level of expression of *AtPTR2-B* in all Arabidopsis organs implies that *AtPTR2-B* has a central role in plant growth and development.

To assess the in vivo role of AtPTR2-B, Arabidopsis plants were transformed with an antisense or sense con-

Table III. *Seed maturation in siliques of T_2 AtPTR2-B transgenics*

Line[a]	Healthy Seed No. per Silique	Aborted Seed No. per Silique	Ratio (Healthy:Aborted)
Wild type	45 ± 6[b]	2 ± 2	22.5:1
pGA941	49 ± 2	3 ± 2	16.3:1
AtPTR2-B antisense			
BA6	25 ± 4	23 ± 4	1:1.1
BA8	13 ± 2	35 ± 5	1:2.6
BA21	14 ± 4	39 ± 8	1:2.9
BA27	21 ± 2	18 ± 5	1.2:1
AtPTR2-B sense			
BS1	38 ± 6	3 ± 3	12.5:1
BS2	21 ± 5	27 ± 9	1:1.2
BS9	34 ± 2	2 ± 2	19.1:1

[a] Siliques were generated from T_2 self-fertilized plants. [b] SD was derived from 10 siliques taken from three independent plants each line.

struct of the *AtPTR2-B* cDNA under the control of the cauliflower mosaic virus 35S RNA promoter. In several transformant lines reduced amounts of *AtPTR2-B* mRNA were found. The reduction in *AtPTR2-B* expression correlated with marked effects on seed development and time of flowering.

As suggested previously, peptide transport may play a nutritional role in seed development (Higgins and Payne, 1982). Thus, we examined seeds collected from wild-type and transgenic plants at different stages of development under the stereomicroscope. The wild-type plant produced normal and healthy seeds, whereas some of the seeds formed by the antisense and BS2 transgenic plants were arrested in development. In the latter case, no differences in seed shape and color were observed in the transgenic siliques before or at the heart stage of embryo development. However, after the heart or torpedo stage, arrested seed development was observed in the transgenic siliques. At this point, some seeds contained green and intact embryos that were easily distinguished from other parts of the seed, whereas the aborted seeds appeared white and empty. After entering the mature cotyledon stage of development, these two types of seeds could be easily separated from each other. The normal seeds appeared as healthy as those in the wild-type siliques, whereas the aborted seeds were much smaller. These observations suggest that the arrest in seed development occurred after the heart or torpedo stage of embryo development and are consistent with the speculation that the peptide transporter may be involved in the import of nitrogen into the embryo, which occurs mainly during the maturation stage of seed development (Bewley and Black, 1986). The reduction in the level of the *AtPTR2-B* transporter as a result of antisense expression might affect the import of nitrogenous nutrients into seeds, thus arresting normal seed development.

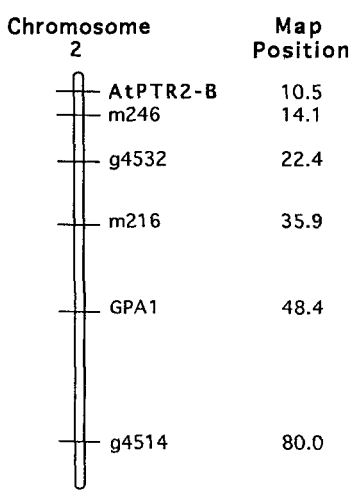

Figure 5. Map position of *AtPTR2-B*. The map position of the *AtPTR2-B* gene was determined using 98 recombinant inbred lines, as described in "Materials and Methods."

Genetic mapping places the AtPTR2B gene at 10.5 cM on chromosome 2, close to the restriction fragment length polymorphism marker m246 at 14.1 cM. A search of the Arabidopsis mutant database revealed the presence of two known embryo defective mutants, *emb34* and *emb93*, that map close to this location. The T-DNA insertional mutant *emb93* maps at 11 cM on chromosome 2 on the classical map (Castle et al., 1993; Franzmann et al., 1995). Embyro development in *emb93* is blocked at the transition from the globular to cotyledon stage of seed development. This phenotype compares favorably to our preliminary analysis of the blockage of seed development in the AtPTR2B antisense lines. The EMS-generated mutant *emb34–1* and the allelic x-ray mutant *emb34–2* map some 4 cM to the other side of marker m246 with respect to AtPTR2B. However, the map positions of both *emb93* and *emb34* are with respect to the classical map and, therefore, their positions may not coincide directly with the map generated with the recombinant inbred lines. Therefore, although the phenotype of the AtPTR2B antisense plants and map location of AtPTR2B close to known embryo defective mutations are an interesting coincidence, more work will be required to show whether these mutants do indeed identify the AtPTR2B locus.

Our previous studies showed that toxic peptides, such as Ala-ethionine and Leu-ethionine, effectively inhibited root growth, and that this inhibition could not be reversed by the addition of amino acids (Steiner et al., 1994), suggesting

that the plant roots must have a peptide transporter. We expected that the antisense *AtPTR2-B* plants would allow us to test the role of this transporter in the uptake of toxic peptides by roots. However, these antisense plants showed little reduction in endogenous *AtPTR2-B* mRNA root expression when compared with the wild-type plants. Consistent with these measurements, root elongation of the sense and antisense plants was inhibited in the presence of the toxic peptide Leu-ethionine (data not shown). Therefore, the transporter mediating toxic peptide uptake in roots remains to be identified. It was a surprising finding that antisense expression of *AtPTR2-B* reduced expression of the endogenous gene in leaves and flowers, but not in roots. However, antisense inhibition is rarely 100% and the degree of inhibition can vary in different tissues (Van der Krol et al., 1988).

The initiation of flowering is a complex process that is regulated by a combination of developmental programs and responses to environmental signals (Lang, 1965; Vince-Prue, 1975). The transition to flowering in Arabidopsis is promoted by long-day photoperiods and vernalization and is also affected by growth temperature, nutrient availability, and light quality (Bowman, 1994). Analysis of various mutants affected in flowering indicates that the transition to flowering may be promoted by more than one pathway (Koornneef et al., 1991). Surprisingly, our transgenic plants exhibited a typical late-flowering phenotype followed by strong leaf growth. This change correlated with the reduced *AtPTR2-B* expression. The delayed flowering seen in the transgenic plants may simply be due to the nutrient defect caused by reduced peptide transport activity. However, the possibility that *AtPTR2-B*-mediated transport may be involved in a pathway that regulates the transition to flowering cannot be excluded.

Received January 13, 1997; accepted March 23, 1997.

LITERATURE CITED

Altmann T, Damm B, Frommer WB, Martin T, Morris PC, Schweizer D, Willmitzer L, Schmidt R (1994) Easy determination of ploidy level in *Arabidopsis thaliana* plants by means of pollen size measurement. Plant Cell Rep **13:** 652–656

An G, Ebert PR, Mitra A, Ha SA (1988) Binary vectors. *In* SB Gelvin, RA Schilperoort, DPS Verma, eds, Plant Molecular Biology Manual. Kluwer Academic Publishers, Dordrecht, The Netherlands, pp 1–19

Andreae WA, Good NE (1955) The formation of indole-acetylaspartic acid in pea seedlings. Plant Physiol **30:** 380–382

Ausubel FM, Brent R, Kingston RE, Moore DD, Seidman JG, Smith JA, Struhl K (1995) Current Protocols in Molecular Biology. Greene Publishing Associates/Wiley Interscience, New York

Becker JM, Naider F (1980) Transport and utilization of peptides by yeast. *In* JW Payne, eds, Microorganisms and Nitrogen Sources. John Wiley and Sons, New York, pp 257–279

Becker JM, Naider F (1995) Fungal peptide transport as a drug delivery system. *In* M Taylor, G Amidon, eds, Peptide Based Drug Design: Controlling Transport and Metabolism. American Chemical Society Books, Washington, DC, pp 369–384

Berlyn GP, Miksche JP (1976) Cytochemistry. *In* GP Berlyn, ed, Botanical Microtechnique and Cytochemistry. Iowa State University Press, Ames, pp 304–307

Bewley JD, Black M, eds (1986) Seeds: Physiology of Development and Germination. Plenum Press, New York

Bowman J (1994) Arabidopsis: An Atlas of Morphology and Development. Springer-Verlag, New York

Brandsch M, Miyamoto Y, Ganapathy V, Leibach F (1994) Expression and protein kinase C-dependent regulation of peptide/H^+ co-transport system in the Caco-2 human colon carcinoma cell line. Biochem J **299:** 252–260

Casadaban MJ, Cohen SN (1980) Analysis of gene control signals by DNA fusion and cloning in *Escherichia coli*. J Mol Biol **138:** 179–207

Castle LA, Errampalli D, Atherton TL, Franzmann LH, Yoon ES, Meinke DW (1993) Genetic and molecular characterization of embryonic mutants identified following seed transformation in *Arabidopsis*. Mol Gen Genet **241:** 504–514

Czako M, An G (1991) Expression of DNA coding for diphtheria toxin chain A is toxic to plant cells. Plant Physiol **95:** 687–692

Damm B, Halfter U, Altmann T, Willmitzer L (1993) Transgenic *Arabidopsis*. *In* SD Kung, R Wu, eds, Transgenic Plants. Academic Press, San Diego, CA, pp 171–186

Dougherty WG, Parks TD (1995) Transgenes and gene supression: telling us something new? Curr Opin Cell Biol **7:** 399–405

Franzmann LH, Yoon ES, Meinke DW (1995) Saturating the genetic map of *Arabidopsis thaliana* with embryonic mutants. Plant J **7:** 341–350

Ganapathy V, Leibach FH (1991) Proton-coupled solute transport in the animal cell plasma membrane. Curr Opin Cell Biol **3:** 695–701

Goodell EW, Higgins CF (1987) Uptake of cell wall peptides by *Salmonella typhimurium* and *Escherichia coli*. J Bacteriol **169:** 3861–3865

Gross DC (1991) Molecular and genetic analysis of toxin production by pathovars of *Pseudomonas syringae*. Annu Rev Phytopathol **29:** 247–278

Heslop-Harrison JS, Maluszyuska J (1994) Molecular cytogenetics of *Arabidopsis*. *In* EM Meyerowitz, CR Somerville, eds, *Arabidopsis*. Cold Spring Harbor Laboratory Press, Cold Spring Harbor, NY, pp 63–87

Higgins CF, Payne JW (1978) Peptide transport by germinating barley embryos: uptake of physiological di- and oligopeptides. Planta **138:** 211–216

Higgins CF, Payne JW (1982) Plant peptides. *In* D Boulder, B Parthier, eds, Encyclopedia of Plant Physiology. Springer-Verlag, New York, pp 438–458

Hood EE, Gelvin SB, Melchers LS, Hoekema A (1993) New *Agrobacterium* helper plasmids for gene transfer. Transgen Res **2:** 208–218

Jamai A, Chollet J-F, Delrot S (1994) Proton-peptide co-transport in broad bean leaf tissues. Plant Physiol **106:** 1023–1031

Klambt HD (1960) Indole-3-acetyl-aspartic acid, a naturally occurring indole derivative. Naturwissenschaften **47:** 398

Koornneef M, Hanhart CJ, Van der Veen JH (1991) A genetic and physiological analysis of late flowering mutants in *Arabidopsis thaliana*. Mol Gen Genet **229:** 57–66

Lang A (1965) Physiology of flowering initiation. *In* W Ruhland, eds, Encyclopedia of Plant Physiology. Springer-Verlag, Berlin, pp 1371–1536

Lister C, Dean C (1993) Recombinant inbred lines for mapping RFLP and phenotypic markers in *Arabidopsis thaliana*. Plant J **4:** 745–750

Manson MD, Blank V, Brade G, Higgins CF (1986) Peptide chemotaxis in *E. coli* involves the Tap signal transducer and the oligopeptide permease. Nature **321:** 253–256

Marton L, Browse J (1991) Facile transformation of *Arabidopsis*. Plant Cell Rep **10;** 235–239

Mathiopoulos C, Mueller JP, Slack FJ, Murphy CG, Patankar S, Bukusoglu G, Sonensgein AL (1991) A *Bacillus subtillis* dipeptide transport system expressed early during sporulation. Mol Microbiol **5:** 1903–1913

Matthews DM (1991) Protein Absorption. Wiley-Liss, New York
Mitchell RE (1976) Isolation and structure of a chlorosis-inducing toxin of *Pseudomonas phaseolicola*. Phytochemistry **15:** 1941–1947
Mitchell RE, Bieleski RL (1977) Involvement of phaseolotoxin in halo blight of beans. Transport and conversion to functional toxin. Plant Physiol **60:** 723–729
Payne JW, Smith MW (1994) Peptide transport by microorganisms. Adv Microbiol Physiol **36:** 1–80
Perego M, Higgins CF, Pearce SR, Gallagher MP, Hoch JA (1991) The oligopeptide transport system of *Bacillus subtillis* plays a role in the initiation of sporulation. Mol Microbiol **5:** 173–185
Rogers SO, Bendich AJ (1985) Extraction of DNA from milligram amounts of fresh, herbarium and mummified plant tissues. Plant Mol Biol **5:** 69–75
Salmenkallio M, Sopanen T (1989) Amino acid and peptide uptake in the scutella of germinating grains of barley, wheat, rice, and maize. Plant Physiol **89:** 1285–1291
Sambrook J, Fritsch EF, Maniatis T (1989) Molecular Cloning: A Laboratory Manual, Ed 2. Cold Spring Harbor Laboratory, Cold Spring Harbor, New York
Song W, Steiner HY, Zhang L, Naider F, Becker JM, Stacey G (1996) Cloning of a second *Arabidopsis* peptide transport gene. Plant Physiol **110:** 171–178
Sopanen T, Burston D, Matthews DM (1977) Uptake of small peptides by the scutellum of germinating barley. FEBS Lett **79:** 4–7
Staskawicz BJ, Panopoulos NJ (1980) Phaseolotoxin transport in *Escherichia coli* and *Salmonella typhimurium* via the oligopeptide permease. J Bacteriol **142:** 474–479
Steel RGD, Torrie JH (1980) Principles and Procedures of Statistics: A Biometrical Approach, Ed 2. McGraw-Hill, New York
Steiner HY, Song W, Zhang L, Naider F, Becker JM, Stacey G (1994) An *Arabidopsis* peptide transport is a member of a new class of membrane transporter proteins. Plant Cell **6:** 1289–1299
Takaiwa F, Oono K, Sugiura M (1984) The complete nucleotide sequence of a rice 17S rRNA gene. Nucleic Acids Res **12:** 5441–5448
Thurmann DA, Street HE (1962) Metabolism of some indole auxins in excised tomato roots. J Exp Bot **13:** 369–377
Van der Krol AR, Lenting PE, Veenstra J, Van der Meer IM, Koes RE, Gerats AGM, Mol JNM, Stuitje AR (1988) An anti-sense chalcone synthase gene in transgenic plants inhibits flower pigmentation. Nature **333:** 866–869
Vince-Prue D (1975) Photoperiodism in Plants. McGraw Hill, London
Walton JD (1990) Peptide phytotoxins from plant pathogenic fungi. *In* H Kleinkauf, HV Dohren, eds, Biochemistry of Peptide Antibiotics. Walter de Gruyter, New York, pp 179–203
Willis DK, Barta TM, Kinscherf TG (1991) Genetics of toxic production and resistance in phytopathogenic bacteria. Experientia **47:** 765–771
Winter A, Thimann KV (1966) Bound indoleacetic acid in *Avena* coleoptiles. Plant Physiol **41:** 335–342